Flood frequency analysis of the Rasina River in Serbia

LJILJANA STRIČEVIĆ[1], NATAŠA MARTIĆ-BURSAĆ[1], MILENA GOCIĆ[1],
NIKOLA MILENTIJEVIĆ[2], MARKO IVANOVIĆ[2]

[1] University of Niš, Faculty of Sciences and Mathematics, Department of Geography, Niš, Serbia; e-mail: ljiljana.stricevic@pmf.edu.rs; natasa.martic-bursac@pmf.edu.rs; milena.gocic@pmf.edu.rs

[2] University of Priština in Kosovska Mitrovica, Faculty of Sciences and Mathematics, Department of Geography, Kosovska Mitrovica, Serbia; nikola.milentijevic@pr.ac.rs; marko.ivanovic@pr.ac.rs

ABSTRACT In this paper we performed flood frequency analysis by using L-moments and annual maximum series data from two hydrological stations on the Rasina River (Brus and Bivolje), for the 1961–2020 period. Homogeneity testing confirmed that the basin can be considered hydrologically homogeneous ($V_i = 0.38 < 1$). Five probability distributions – Normal, Log-Normal, Gumbel, Pearson Type III, and Log-Pearson Type III – were tested to identify the best-fit model. An L-moment ratio diagram and *Z*-statistics indicate that all distributions satisfy the test criteria, with Log-Pearson Type III showing the best overall fit for the region ($Z = 0.09$). Goodness-of-fit tests (Kolmogorov-Smirnov, Cramér-von Mises, and χ^2) confirmed Log-Pearson Type III as the best fit at the Brus station and Pearson Type III at the Bivolje station. Theoretical flood quantiles were calculated for various return periods (T-year floods). Mann–Kendall trend analysis indicated a significant decreasing discharge trend at Bivolje (–1.28 m³/s per year).

KEY WORDS flood frequency analysis – L-moments – Rasina River

STRIČEVIĆ, L., MARTIĆ-BURSAĆ, N., GOCIĆ, M., MILENTIJEVIĆ, N., IVANOVIĆ, M. (2026): Flood frequency analysis of the Rasina River in Serbia. Geografie, 131, 1, 1–26.
https://doi.org/10.37040/geografie.2026.002
Received July 2025, accepted February 2026.

Introduction

Floods are among the most frequent and destructive natural disasters worldwide, both in terms of recurrence and the magnitude of their socio-economic and environmental impacts. They pose significant threats to human life, infrastructure, ecosystems, and economic development (Jonkman, Curran, Bouwer 2024; Ionita, Nagavciuc 2021). According to the United Nations Office for Disaster Risk Reduction (UNDRR 2025), floods account for approximately 35–40% of all natural hazard-related events globally.

In the European Economic Area, weather-related disasters have caused estimated economic losses of €487 billion between 1980 and 2020 (Snizhko et al. 2023). Future climate scenarios suggest an increase in the frequency and intensity of extreme precipitation events, further exacerbating flood risks (Alfieri et al. 2017).

Although extensive research has addressed the spatial and temporal variability of hydrological extremes, no uniform global trends have been established (Varlas et al. 2023; Kovačević-Majkić, Urošev 2014). In Europe, several studies have explored flood seasonality, frequency, and long-term trends (Lehmkuhl et al. 2022; Bloschl et al. 2019; Tramblay et al. 2019; Alfieri et al. 2016; Arnell, Gosling 2014). In northwestern Europe, rising flood frequency is mainly attributed to increased heavy precipitation. In contrast, southern Europe has experienced a decline in flood hazard due to reduced precipitation and drier soils, while eastern Europe has seen similar trends due to less intense snowmelt (Bertola et al. 2020). Regional variation is also reflected in flood timing: in eastern Europe floods are more typical in late March, while in mountainous regions maximum flows often occur in early summer (Hall, Bloschl 2018; Parajka et al. 2010). In the Mediterranean, annual streamflow volumes have consistently remained below the 1950–2013 average since the early 1980s (Masseroni et al. 2021).

In Serbia, floods are the most frequent natural hazard, accounting for 53% of disaster events (Milanović-Pešić 2020). Approximately 18% of the national territory is classified as flood-prone area (Gavrilović, Milanović-Pešić, Urošev 2012). The most vulnerable areas include Vojvodina and the Posavina and Pomoravlje regions, particularly along the Sava and Velika Morava Rivers (Gavrilović, Dukić 2002). Flood events in Serbia are commonly caused by moist Atlantic air masses or rapid snowmelt from the Dinaric Alps, with peak flows occurring in late spring and early summer (Leščešen et al. 2022).

One of the most pressing challenges in hydrology is the reliable estimation of extreme flood events (Leščešen, Dolinaj 2019). Flood Frequency Analysis (FFA) is widely used to estimate discharges associated with specific return periods, applying statistical distributions to observed data (Hu et al. 2023). Over the past several decades, many studies have been conducted on FFA across various regions and hydrological contexts (Shah, Pan Das 2024; Fischer, Schumann 2021; Morlot,

Brilly, Šraj 2019; Engeland et al. 2018; Dubey 2014; Noto, La Loggia 2009). The main goal of this research is to provide practical tools for flood estimation to inform flood engineering designs, as well as to provide a better understanding of flood characteristics.

Numerous researchers have examined the issue of flooding on rivers in Serbia through the application of FFA (Gnjato et al. 2025; Leščešen et al. 2022; Leščešen, Dolinaj 2019), as well as through analyses of high-flow conditions and major historical flood events (Gavrilović, Milanović-Pešić, Urošev 2012; Gavrilović 1981). Research has also focused on flood risk assessment and hydrological changes, with an emphasis on statistically significant long-term trends and seasonal variability in water resources (Stričević, Martić-Bursać, Gocić 2024; Leščešen et al. 2022; Stojković et al. 2017; Martić-Bursać et al. 2016; Kovačević-Majkić, Urošev 2014).

Accurate flow forecasting is crucial for water resource management, infrastructure planning, and operational decision-making (Samantaray, Sahoo 2020). Flood frequency analysis (FFA) provides essential estimates of flood magnitude and frequency for risk assessment and engineering design (Shah, Pan Das 2024; Ahmad et al. 2016), relying on long-term, high-quality peak discharge data (Hu et al. 2023). Commonly used statistical distributions in FFA include Normal (N), Log-Normal (LN), Gumbel (GUM), Generalized Extreme Value (GEV), Pearson Type III (PIII) and Log-Pearson Type III (LPIII) distributions. Different countries have adopted specific distributions for national applications – for example, the GEV in Europe (Kousar et al. 2020), LPIII in the United States (England et al. 2019), GEV and PIII in Australia (Rahman et al. 2013).

Although FFA has been widely applied in Serbia and Europe, most studies focus on major rivers or regional-scale assessments, while small catchments like the Rasina River Basin remain less investigated (Stričević, Martić-Bursać, Gocić 2024; Leščešen et al. 2022). Flood trends and methodological results vary due to differences in hydrological regimes and data availability (Bertola et al. 2020; Alfieri et al. 2016). The L-moments method was selected for its robustness with limited sample sizes and reliability in characterizing extreme events (Dubey 2014; Hosking, Wallis 1997), allowing this study to provide dependable estimates of extreme discharges in small Serbian catchments. This study focuses on the Rasina River basin in central Serbia, analyzing discharge data from two hydrological stations – Brus and Bivolje – for the period 1961–2020. The Brus station represents a near-natural streamflow regime, while Bivolje is influenced by the Ćelije Reservoir, located in the Zlatar Gorge. As extreme floods in the Rasina River are expected to become more frequent due to climate change, a reliable FFA is essential for engineering applications. Therefore, this study focuses on the estimation of extreme river discharges.

The main objectives of the study are to: assess the hydrological homogeneity of the Rasina River Basin; estimate regionalized flood parameters using the

L-moments method; identify the best-fitting probability distribution for modeling flood magnitudes; detect trends in annual maximum discharges using the Mann–Kendall (MK) test.

The broader aim of this research is to emphasize the need for comprehensive flood analyses in small catchments across Serbia in order to enhance flood prediction capabilities and support the implementation of effective mitigation strategies.

Study area

The basin of the Rasina River is situated in the south part of the middle Serbia connecting the Dinaric and Serbian – Macedonian masses (Fig. 1). The Rasina is formed on the east and south-east slopes of the mountains of Goč, Željin and Crni Vrh, where its constituents, the Vranjuša and the Burmanska River originate. These streams merge near Rogavčina, forming the Rasina River, which flows into the Zapadna Morava River after 92.3 km, approximately 5 km downstream from Kruševac, at an altitude of 134 m a.s.l. (Dimitrijević 2010). The basin covers an area of 979.6 km², representing 6.18% of the Zapadna Morava basin (Stričević 2015).

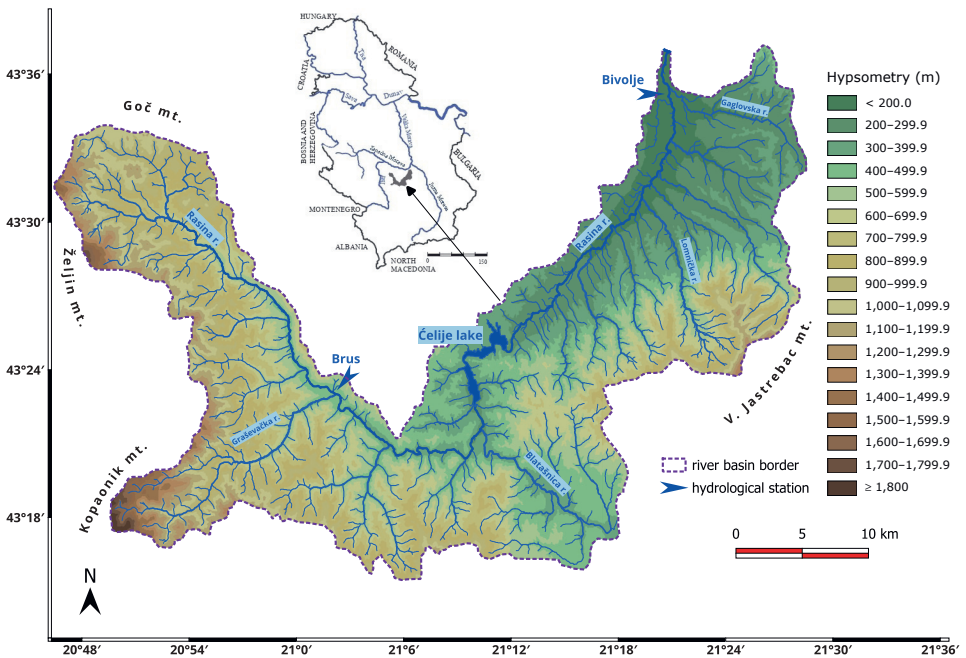

Fig. 1 – Geographical position of the research area and hydrological stations Brus and Bivolje in the Rasina River basin. Source: QGIS software with 30 m SRTM DEM (USGS EarthExplorer).

The river network comprises 955 watercourses, with a drainage density of 1.383 km/km². The largest tributaries are the Grošnička River and Blatašnica on the right side and the Zagrža on the left. Average discharge of the Rasina River in the period from 1961 to 2020 was 7.37 m³/s, which gave the specific runoff of 7.52 l/s/km².

The elevation ranges from 134 m to 1,934 m a.s.l., with a mean altitude of 590.9 m. About 45.3% of the basin area lies below 500 m, 41.2% between 500 and 1,000 m, and 13.5% above 1,000 m a.s.l. (Dimitrijević 2010). The largest part of the Rasina River basin is situated in the zone of temperate continental climate with continental pluviometric regime, while mountainous climate is represented on the mountain edge of the basin. In the north, the basin is widely open towards Župa and the valley of the Zapadna Morava, from where continental air masses penetrate unhindered. The average annual air temperature in the basin is 8.9 °C and mean annual precipitation amounts to 794 mm. Approximately 30% of precipitation contributes to runoff (runoff coefficient 0.30), with the highest values recorded in spring (0.48) and the lowest in summer (0.15). According to the Corine Land Cover database (2012) agricultural areas cover 32% of the basin, mainly at lower altitudes near river valleys and settlements, while forests and semi-natural areas occupy 58%. According to the 2021 census (Statistical Office of the Republic of Serbia – SORS 2021), this territory has a total population of 154,659, distributed across two urban and 211 rural settlements.

In 1972, Lake Ćelije was created by damming the Rasina River in the Zlatar Gorge, approximately 33 km upstream from its confluence with the Zapadna Morava River. The reservoir serves multiple purposes, including flood control and flow regulation, significantly reducing flood intensity and frequency in the downstream river section (Vujović 1995).

Data and methods

Flood frequency analysis (FFA) of the Rasina River basin was conducted by using annual maximum series (AMS) data, which consist of the largest discharge event recorded each year. The AMS method is widely used in hydrological practice due to its simplicity and the relatively low data requirements for estimating statistical distributions (Anghel, Ilinca 2023; Ilinca, Anghel 2022; Leščešen et al. 2022; Anwat et al. 2021; Bezak, Brilly, Šraj 2016; Urošev et al. 2016). In this study, a 60-year dataset (1961–2020) of AMS discharge values from two gauging stations (Brus and Bivolje) on the Rasina River, was analyzed. The data were obtained from the Republic Hydrometeorological Service of Serbia (RHMSS). The locations of the stations are shown in Figure 1, and their main geographical parameters are summarized in Table 1. The research area was visualized using QGIS 3.40 and SAGA GIS

with a 30 m SRTM DEM (USGS EarthExplorer) and the station locations were obtained from RHMSS.

FFA enables the estimation of future flood magnitudes and return periods, particularly useful in regions with similar climatic and hydrological conditions. Numerous studies have been focused on identifying suitable probability distribution functions for modeling annual maximum flood events (Sahu, Kant Verma, Ahmad 2022; Radevski, Gorin 2017; Vasilevski, Radevski 2014). While there is no strict rule for selecting a specific distribution for short-term AMS data, this study evaluated five commonly used distributions: Normal (N), Log-Normal (LN), Gumbel (GUM), Pearson Type III (PIII), and Log-Pearson Type III (LPIII). These distributions were applied to model flood magnitudes at the two gauging stations. The probability density functions (PDF) and quantile functions y(*F*) for each distribution are presented in Table 2 (Gnjato et al. 2025; Anghel, Ilinca 2023; Deraman, Abd Mutalib, Mukhtar 2017).

Goodness-of-fit was evaluated using statistical tests: Chi-square (χ^2), Cramér–von Mises (CvM), and Kolmogorov–Smirnov (K–S), as well as graphical assessments. The fitted distributions were used to estimate discharge values for various return periods (5, 10, 15, 50 years, etc; Fischer, Schumann 2021; Acharya, Joshi 2020; Deraman, Abd Mutalib, Mukhtar 2017; Smith, Sampson, Bates 2015). The corresponding cumulative distribution functions (CDFs) are also presented to illustrate the flood probabilities associated with different magnitudes.

The first step in FFA is to determine the level of regional homogeneity (Gnjato et al. 2025; Leščešen et al. 2022; Leščešen, Dolinaj 2019). To identify the homogeneity of the study area, a homogeneity test was first applied to stations data in the Rasina River basin. For quantitative evaluation, Hosking, Wallis (1993) proposed a homogeneity test statistic and a goodness-of-fit statistic for determining the regional distribution. The homogeneity test checks whether the selected group of stations can be considered a random realization of the same dimensionless distribution in terms of L-Cv (V_1), L-Cv and L-Cs (V_2) and L-Cs and L-Ck (V_3). V_1 represents the Euclidean distance between the L-Cv values for each station individually and the regional mean L-Cv, while V_2 and V_3 represent the distances in L-Cs–L-Cv and L-Ck–L-Cs, respectively. For the sample and simulated regions, V_i is calculated as:

$$V_1 = \left\{\sum_{i=1}^{n} n_i\left(\tau^i - \tau^R\right)^2 / \sum_{i=1}^{n} n_i\right\}^{1/2} \quad (1)$$

$$V_2 = \left\{\sum_{i=1}^{n} n_i\left(\tau^i - \tau^R\right)^2 + \left(\tau_3^i - \tau_3^R\right)^2\right\}^{1/2} / \sum_{i=1}^{n} n_i \quad (2)$$

$$V_3 = \left\{\sum_{i=1}^{n} n_i\left(\tau_3^i - \tau_3^R\right)^2 + \left(\tau_4^i - \tau_4^R\right)\right\}^{1/2} / \sum_{i=1}^{n} n_i \quad (3)$$

where n is the number of sites; n_i is the record length at site i; τ^i, τ_3^i, τ_4^i are the sample L-Cv, L-Cs, L-Ck at site i; n_i is the record length at site i; τ^R, τ_3^R, τ_4^R are the

Table 1 – Geographical characteristics for observed stations

Station	Elevation (m a.s.l.)	Location (River-km)	Basin Area (km²)
Brus	417.9	69.96	213
Bivolje	141.9	5.97	958

Table 2 – Probability density and quantiles functions of the probability distributions

Distribution	Probability density function f(x)	Quantile function F(x)
Normal	$f(x) = \frac{exp\left(-\frac{1}{2}\left(\frac{x-\mu}{\sigma}\right)^2\right)}{\sigma\sqrt{2\pi}}$	$F(x) = \varphi\left(\frac{x-\mu}{\sigma}\right)$
Log-Normal	$f(x) = \frac{exp\left(-\frac{1}{2}\left(\frac{\ln x-\mu}{\sigma}\right)^2\right)}{x\sigma\sqrt{2\pi}}$	$F(x) = \varphi\left(\frac{\ln x-\mu}{\sigma}\right)$
Gumbel	$f(x) = \frac{1}{\sigma}exp\left(-z - exp(-z)\right)$	$F(x) = exp\left(-exp(-z)\right)$
Pearson III	$f(x) = \frac{1}{\beta^{\alpha}\Gamma(\alpha)}(x-\mu)^{\alpha-1}exp\left(-\frac{(x-\mu)}{\beta}\right)$	Explicit analytical form is not available
Log-Pearson III	$f(x) = \frac{1}{X\lvert\beta\rvert\Gamma(\alpha)}\left(\frac{\ln(x)-\gamma}{\beta}\right)^{\alpha-1} exp\left(-\frac{\ln(x)-\gamma}{\beta}\right)$	$F(x) = \frac{\Gamma_{\ln((x)-\gamma)/\beta\ \ (\alpha)}}{\Gamma(\alpha)}$

Table 2a – Explanation of symbols used in Table 2

Symbol	Explanation	Symbol	Explanation
x	Value of the random variable (discharge)	β	Scale parameter for Pearson III and Log-Pearson III distributions
X	Random variable representing discharge	γ	Location parameter for Log-Pearson III distribution
μ	Mean or location parameter of the distribution	$f(x)$	Probability density function (PDF)
σ	Standard deviation or scale parameter of the distribution	$F(x)$	Cumulative distribution function (CDF) or Quantile function
z	Standardized variable for Gumbel distribution: $z = \frac{x-\mu}{\sigma}$	$\varphi(\cdot)$	Standard normal cumulative distribution function (CDF)
α	Shape parameter for PIII and LPIII distributions	$\Gamma(\cdot)$	Gamma function

sample L-moments at site i, corresponding to the coefficients L-Cv (L-moment coefficient of variation), L-Cs (L-moment skewness), and L-Ck (L-moment kurtosis), respectively; and τ^R, τ_3^R, τ_4^R are the corresponding regional average L-moments. The region is regarded as "acceptably homogeneous" if $V_i < 1$, "possibly heterogeneous" if $1 \leq V_i < 2$ and "definitely heterogeneous" if $V_i \geq 2$ (Hosking,Wallis 1997).

The L-moments method was used to estimate distribution parameters (Khan, Rahman, Karim 2023). The most commonly employed method to calculate the L-moments is via probability weighted moments (PWMs). PWMs primarily were defined by Greenwood et al. (1979), and later by Hosking (1990):

$$\beta_r = E\{X[F(x)]^r\} \tag{4}$$

where, β_r is the r^{th} order PWMs and $F(x)$ characterizes the CDFs of x. Sample estimators (β_i) of the first four PWMs are explained in Hosking, Wallis (1997):

$$\beta_0 = m = \frac{1}{n}\sum_{j=1}^{n} X_j \tag{5}$$

$$\beta_1 = \sum_{j=1}^{n-1}\left(\frac{n-j}{n(n-1)}\right)X_j \tag{6}$$

$$\beta_2 = \sum_{j=1}^{n-2}\left(\frac{(n-1)(n-j-2)}{n(n-1)(n-2)}\right)X_j \tag{7}$$

$$\beta_3 = \sum_{j=1}^{n-3}\left(\frac{(n-j)(n-j-1)(n-j-2)}{n(n-1)(n-2)(n-3)}\right)X_j \tag{8}$$

where X_j represents the j^{th} value of the AMS arranged in descending order, so with X_1 is the largest and X_n the smallest. Regarding PWMs, the initial four L-moments, signifying the mean, scale, skewness, and kurtosis of the distributions, are established through linear combinations of PWMs (Hosking, Wallis 1997):

$$\lambda_1 = \beta_0 \tag{9}$$
$$\lambda_2 = 2\beta_1 - \beta_0 \tag{10}$$
$$\lambda_3 = 6\beta_2 - 6\beta_1 + \beta_0 \tag{11}$$
$$\lambda_4 = 20\beta_3 - 30\beta_2 + 12\beta_1 - \beta_0 \tag{12}$$

Finally, the L-moment ratios defined by Hosking, Wallis (1993) are specified below:

$$LC_v = \tau_2 = \frac{\lambda_2}{\lambda_1} \tag{13}$$

$$LC_s = \tau_3 = \frac{\lambda_3}{\lambda_2} \tag{14}$$

$$LC_k = \tau_4 = \frac{\lambda_4}{\lambda_2} \tag{15}$$

where τ_2 is the L coefficient of variation, τ_3 is the L coefficient of skewness, τ_4 is the L coefficient of kurtosis.

To identify the distribution that yields the most accurate quantiles, the widely accepted L-moment ratio diagram method was applied (Fig. 3). This method is widely recognized for selecting the best-fit probability distribution for regional datasets (Ilinca, Anghel 2022; Anderson 2019).

The appropriate distribution is selected by comparing the proximity of sample L-Cs and L-Ck values to the theoretical curves of candidate distributions (in

the case of three-parameter distributions), or by comparing the sample mean to theoretical points (for two-parameter distributions) (Domanski et al. 2023; Gielczewski, Piniewski, Domanski 2022; Ahmad et al. 2016). If the region is homogeneous, sample points on the L-moment ratio diagram tend to cluster closely.

However, when several distributions appear suitable, the L-moment diagram alone may not clearly indicate the best fit. Therefore, a numerical goodness-of-fit test is applied to objectively determine the most appropriate frequency distribution. In this study, the *Z*-statistic was used as the goodness-of-fit measure for identifying the most appropriate regional distribution (Sahu, Kant Verma, Ahmad 2022; Zakaria, Shabri 2013). It is based on the comparison of sample- and population-L-Ck values for the different distributions:

$$Z = \left(\tau_4^{DIST} - \tau_4^R\right)/\sigma_4 \tag{16}$$

where σ_4 is the standard deviation of the sample L-Ck values, τ_4^{DIST} is the population-L-Ck value for a particular candidate distribution, τ_4^R is the regional sample average of the L-Ck values (Ahmad et al. 2019). The test is performed by means of a comparison with a quantile of the standard normal distribution. We adopted a significance level of 5%, which means that a candidate distribution is considered suitable if $|Z| < 1.96$. The best fit to the observed data indicates the most appropriate distribution (Leščešen, Dolinaj 2019; Ahmad et al. 2016).

For clarity, CDFs chart was created to further validate the results and strengthen their credibility (Figure 4). This diagram visually compares the distribution of observed discharge values with those estimated using different probability distributions (Anderson 2019). The *x*-axis represents the cumulative probability of occurrence, while the *y*-axis represents the discharge values. The empirical cumulative probabilities $F_e(x)$ were calculated using the Weibull plotting position formula:

$$F_e(x) = \frac{m}{N+1}$$

where m is the rank of the observation in ascending order (the smallest value $m = 1$) and N is the total number of observations (Hosking, Wallis 1997). This method provides an unbiased estimation of empirical probabilities, particularly suitable for extreme value analysis.

The uncertainty of trend and return level estimates is expressed by 95% confidence intervals. For trend analysis (Fig. 2), confidence limits were derived for Sen's slope, whereas for return levels (Figure 5 and 6) they were obtained from L-moment–based quantile estimation.

The best-fitting distribution function for the 60-year data series was determined using K–S, CvM and χ^2 tests (Petrović, Leščešen, Radevski 2024; Martinenko et al. 2021; Kousar et al. 2020; Urošev et al. 2016). The K-S test is a frequently employed method for assessing the consistency of probability distribution, delivering

reliable results even with limited sample data. The approach involves computing the value of D_{max}, the maximum unconditional deviation between the cumulative extent of two distributions, followed by comparison with the critical value of D to either accept or reject the proposed hypothesis (Kovačević, Marković, Babić 2014). When comparing multiple theoretical distributions, the one with the lowest D_{max} is considered the best fit to the empirical data. The K-S test goes as follows:

$$D_{max} = |F_e(x) - F_t(x)| \tag{17}$$

where $F_e(x)$ is the empirical cumulative distribution function (observed data) and $F_t(x)$ is the theoretical cumulative distribution function (candidate distribution).

Similarly, the CvM test evaluates the concordance between empirical and theoretical distributions. The test statistic w^2 is calculated as:

$$w^2 = \frac{1}{12N} + \sum_{i=1}^{N} |F_e(x) - F_t(x)|^2 \tag{18}$$

where N is the number of observations. Smaller values of w^2 indicate closer conformity to the empirical data. To check the agreement of the empirical and theoretical distribution of flood occurrence rates the test χ^2 was used:

$$\chi^2 = \sum_{k=1}^{k} \frac{(f_{e,k} - f_{t,k})^2}{f_{t,k}} \tag{19}$$

where $f_{e,k}$ is the empirical frequency in class k, $f_{t,k}$ is the theoretical frequency in class k, and K is the number of classes of the random variable. The degrees of freedom for the χ^2 statistic are calculated as $\upsilon = K - p - 1$, where p is the number of parameters of the fitted distribution. The analyzed data are grouped in six classes, so that each class comprises of at least five data points.

The critical value $\chi^2_{1-\alpha}$ is obtained from standard Chi-squared tables for the given degrees of freedom υ and significance level α. If $\chi^2 < \chi^2_{1-\alpha}$, the hypothesis of agreement between empirical and theoretical distributions is accepted.

The statistical significance of the trend in maximum series was analyzed using the non-parametric Mann–Kendall (MK) test (Kendall 1975; Mann 1945). The MK test is widely used to detect a statistically significant trend in hydrological and climatic variables, particularly in streamflow series (Higashino, Stefan 2019; Radevski et al. 2018; Bezak, Brilly, Šraj 2016; Kovačević-Majkić, Urošev 2014). The magnitude of the trend was determined by using Sen's slope test (Sen 1968), which examines the sign differences between earlier and later data points. The null hypothesis H_0 assumes no trend, while the alternative H_1 assumes a monotonic trend. First, we calculated sign differences S, after that variance $\mathrm{Var}(S)$, and in the end MK test statistic Z_t.

The Mann–Kendall statistics and its variance can be presented as:

$$S = \sum_{i=1}^{n-1} \sum_{j=i+1}^{n} sgn(X_j - X_i) \tag{20}$$

$$sgn(X_j - X_i) = \begin{bmatrix} 1, \text{if } (X_j - X_i) > 0 \\ 0, \text{if } (X_j - X_i) = 0 \\ -1, \text{if } (X_j - X_i) < 0 \end{bmatrix} \tag{21}$$

$$\text{Var}(S) = \frac{n(n-1)(2n+5) - \sum_{k=1}^{n} t_k(t_k-1)(2t_k+5)}{18} \tag{22}$$

The standardized statistics Z_t for this test can be calculated by the following equation:

$$Z_t = \begin{bmatrix} \frac{S-1}{\sqrt{\text{Var}(S)}}, \text{if } S > 0 \\ 0, \text{if } S = 0 \\ \frac{S+1}{\sqrt{\text{Var}(S)}}, \text{if } S < 0 \end{bmatrix} \tag{23}$$

where n is the total length of data, X_j and X_i are the time series of the annual and/or seasonal values of the discharge in years $j = i + 1, i + 2, i + 3, \ldots, n$ and $i = 1, 2, 3, \ldots, n - 1$, where $j > i$, and n is the last year in the time series, while t_k is the number of data in the k-th tied group.

The positive values of Z_t indicate upward (increasing) trends in time series, and the negative values show downward (decreasing) trends. Trends (Z_t statistics) are then tested against some critical values ($Z_{t\,1-\alpha}$) to show whether they are statistically significant or not. If α is the Type I error rate, where $0 < \alpha < 0.5$, and $Z_{t\,1-\alpha}$ is the $1-\alpha$ quantile of the standard normal distribution (provided in statistical books or statistical software packages), then H_0 will be rejected, and replaced with the alternative H_1 if $Z_t \geq Z_{t\,1-\alpha}$ for the upward, or $Z_t \leq -Z_{t\,1-\alpha}$ for the downward trend.

Results and discussion

The first step was to calculate the basic statistics of the AMS data (mean, median, maximum, standard deviation, skewness and kurtosis) for the two gauging stations. The positive skewness values indicate that the AMS data at these stations deviate from a normal distribution (exhibiting right skewness; Table 3). These basic statistics were then used to select the frequency distributions for deriving the probability of exceeding a certain discharge value (Leščešen et al. 2022).

Trend analysis of the AMS data at the two gauging stations is presented in Figure 2. To determine a trend, the MK test was applied. At the Bivolje station, a statistically significant decreasing trend was detected ($p = 0.005$), significant at 0.1, 0.05, and 1% levels, but not at the more stringent level of 0.001. The Sen's slope of –1.28 m³/s/year indicates an average annual decrease in discharge of approximately 1.28 m³/s (Table 4). The standard error of 0.38 suggests relatively good precision of the slope estimate. In contrast, data from the Brus station show

Table 3 – Descriptive statistics for the AMS data from the two gauging stations on the Rasina River

Station	n	Mean (m^3/s)	Median (m^3/s)	Maximum (m^3/s)	STD (m^3/s)	Skewness	Kurtosis
Brus	60	32.14	22.9	121	24.57	0.42	0.25
Bivolje	60	103.11	86	291	71.79	0.25	0.05

n – number of observations; STD – standard deviation; Skewness – coefficient of skewness; Kurtosis – coefficient of kurtosis

Table 4 – Man–Kendall test statistics for the Rasina River

Station	Sen's slope $m^3/s \cdot year^{-1}$	SE $m^3/s \cdot year^{-1}$	Z_t-value of trend	p-value
Brus	–0.027	0.098	–0.204	0.838
Bivolje	–1.279	0.383	–2.787	0.005

Sen's slope – magnitude of monotonic trend estimated by Sen's method; SE – standard error of Sen's slope; Z_t-value – standardized test statistic of the Mann–Kendall test; p-value – significance level of the trend

no statistically significant trend in annual maximum discharges ($p = 0.838$). Sen's slope is very close to zero (–0.027), indicating a practically negligible decreasing trend. Therefore, while a significant declining discharge trend was established at Bivolje, which may have implications on water supply and water resource management, discharges at Brus remained stable over the observed period with no evidence of trend change. The negative trends may result from reduced snowmelt in surrounding mountains (Kopaonik, Goč, Željin, Jastrebac), the main sources for right-bank tributaries. The presented results are consistent with other studies, which project decreasing discharge trends for major rivers in Serbia, as well as in central and southern Europe (Leščešen et al. 2022; Stagl, Hattermann 2015; Kovačević-Majkić, Urošev 2014).

Homogeneity test results for the Rasina River basin are presented in Table 5. Based on these results, it can be concluded that the study region is acceptably homogeneous, as all V_i values are below the critical threshold of one, and no further data inspection is necessary.

Once regional homogeneity is confirmed, regional L-moments were calculated as the weighted average of the L-moments from the two gauging stations (Dubey 2014). These regional L-moments were computed across all gauging stations, with weights corresponding to the record length at each station. This ensures that longer records contribute proportionally more to the regional estimates, providing a more reliable basis for distribution selection. Figure 3 shows a scatter plot of observed L-moments for the two gauging stations (Brus and Bivolje), with lines for theoretical distributions, highlighting the best-fitting one. Since the sample L-moments are unbiased, the sample points should be distributed both above and below the theoretical line of the fitted distribution (Sahu, Kant Verma,

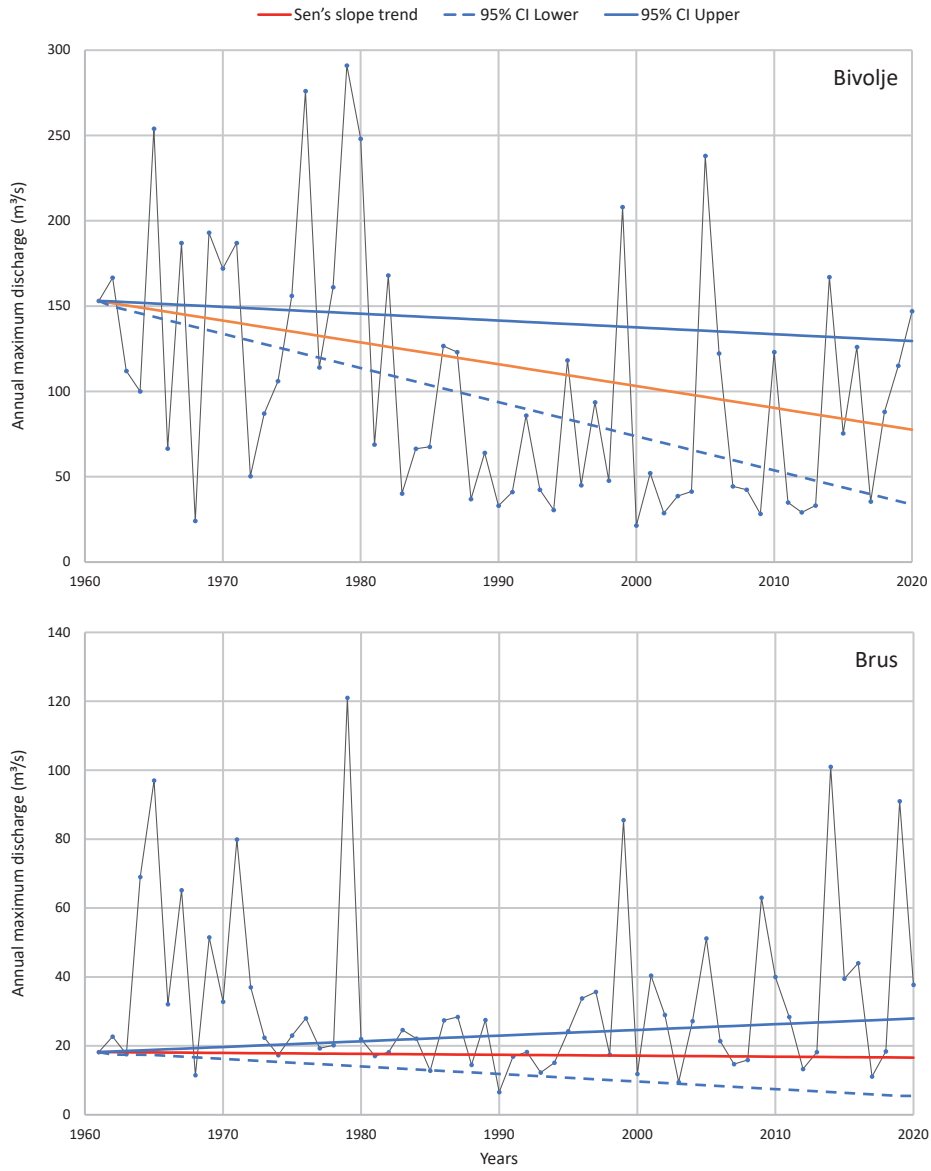

Fig. 2 – Time series of maximum annual discharges at the Rasina River from 1961 to 2020 at Bivolje (up) and Brus (down)

Ahmad 2022). The L-Cv values for the region were between 0.37 and 0.39, with a mean value of 0.38. The L-Cs range was between 0.25 and 0.42, with a mean value of 0.33; whereas the L-Ck range was 0.05 and 0.25, with a mean value of 0.15. The results show that there is no clear variation of L-Ck and L-Cs within the basin.

Table 5 – Homogeneity test of the Rasina River for flood volumes

τ^R	τ_3^R	τ_4^R	V_1	V_2	V_3
0.986	0.986	0.987	0.0058	0.0155	0.0173

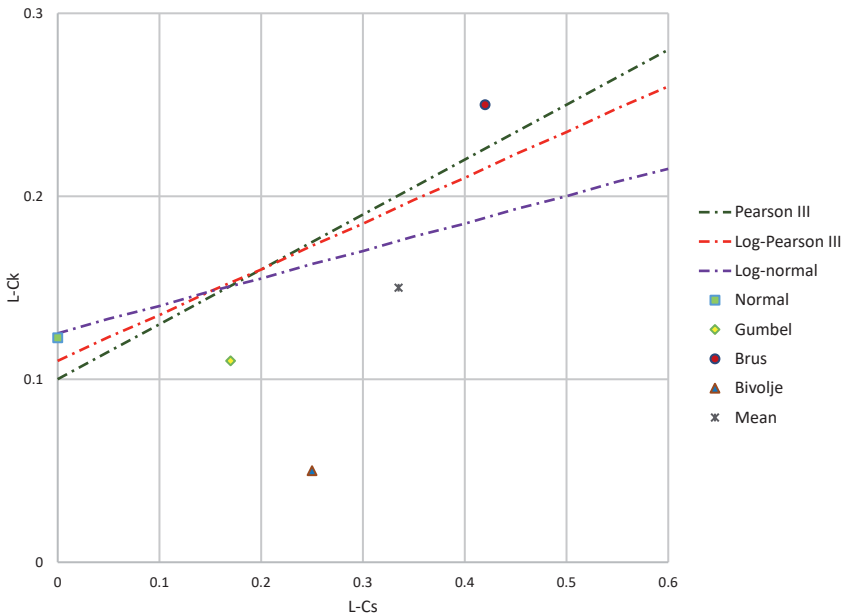

Fig. 3 – Scatter plot of observed L-moments for the two selected gauging stations (Brus and Bivolje, 1961–2020) in the Rasina River basin, with lines for theoretical distributions

Most data points display a tendency to group around the PIII and LPIII distribution functions. Figure 3 indicate that the PIII and LPIII distributions provide the best fit to the observed AMS data for the Brus and Bivolje stations (Amirataee, Montaseri 2013).

To identify a regional distribution applicable to ungauged rivers, the *Z*-statistic was calculated. The results show that the *Z*-statistic for all five distributions is less than the critical value ($|Z|$): Normal ($Z = -0.13$), Log-Normal ($Z = 1.11$), Gumbel ($Z = 0.25$), Pearson III ($Z = 0.23$), and Log-Pearson III ($Z = 0.09$). Since the absolute value of *Z* for the Log-Pearson III distribution is the lowest, this provides additional evidence that this distribution is suitable for the Rasina River basin as a whole.

In order to examine the goodness-of-fit of the selected distribution to the empirical data, the CDF were calculated for the analyzed hydrological stations (Figure 4). This diagram visually compares the distribution of observed discharge values with those estimated using different probability distributions. The *x*-axis

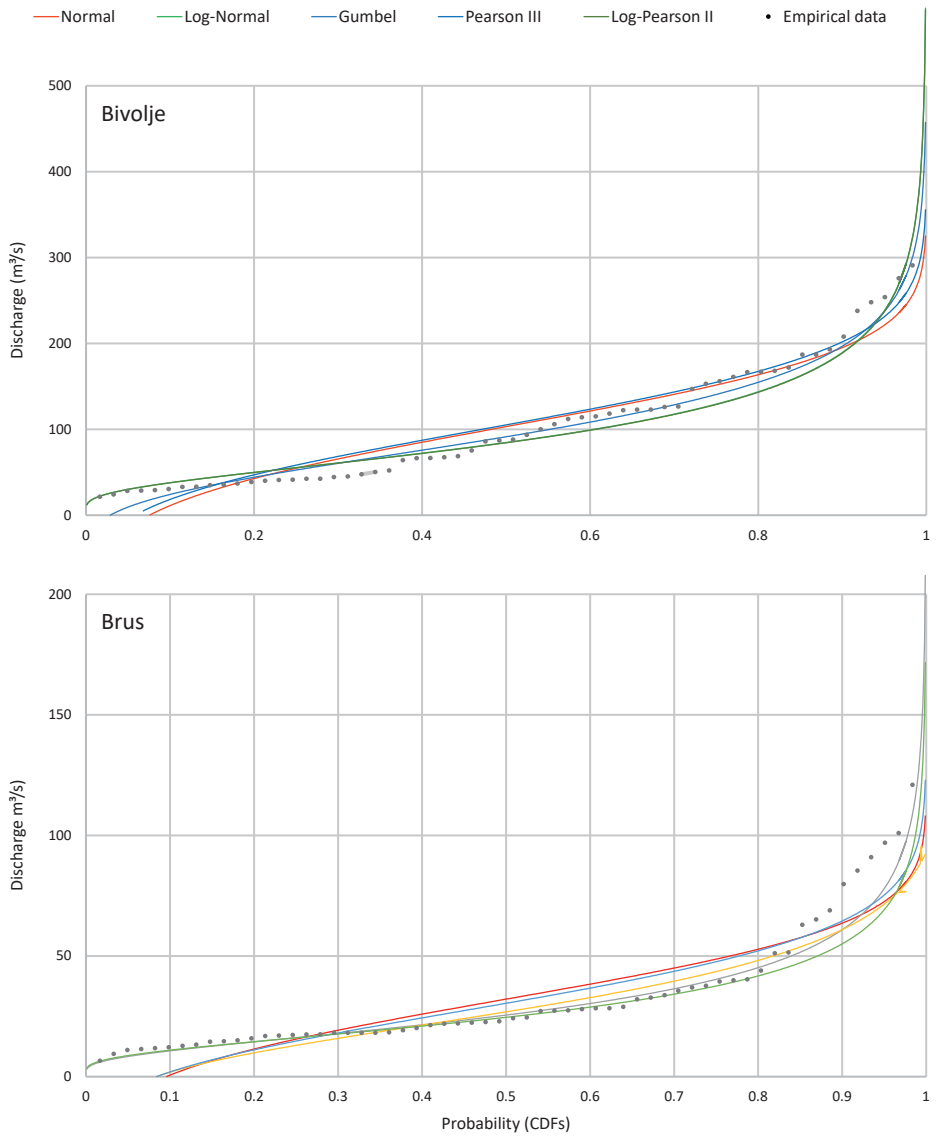

Fig. 4 – CDFs of empirical data and fitted candidate distributions for the stations Brus and Bivolje in the Rasina River basin

represents the cumulative probability of occurrence, while the y-axis indicates the discharge values. The CDF diagram shows that the Normal distribution deviates significantly from the observed discharge values, indicating a lack of fit. In contrast, other distributions show a considerable overlap with the observed discharge data, indicating a better fit. Figure 4 shows thatPIII and LPIII distributions have

Table 6 – Fit statistics and distribution selection for river discharge data

Station	Distribution	Goodness-of-Fit Test					
		K–S		CvM		χ^2	
		Stat.	p-value	Stat.	p-value	Stat.	p-value
Brus	Normal	0.217	0.007	0.844	0.006	29.452	0
	Log-Normal	0.097	0.628	0.121	0.492	2.642	0.619
	Gumbel	0.087	0.753	0.389	0.077	11.932	0.018
	Pearson III	0.111	0.453	0.091	0.633	5.992	0.199
	Log-Pearson III	0.063	0.973	0.030	0.977	2.081	0.721
Bivolje	Normal	0.141	0.186	0.278	0.156	20.033	0.0004
	Log-Normal	0.113	0.430	0.159	0.363	7.489	0.112
	Gumbel	0.121	0.341	0.151	0.388	9.911	0.042
	Pearson III	0.100	0.582	0.107	0.554	5.176	0.270
	Log-Pearson III	0.108	0.490	0.134	0.442	5.754	0.218

the best fit for the entire range of empirical data. Similar results for best-fit distributions have been obtained in Serbia for the Danube River (Urošev et al. 2016), the Kolubara River (Milanović-Pešić 2020), as well as for major tributaries of the Južna Morava (e.g., Vlasina) and Velika Morava Rivers (e.g., Jasenica, Lepenica) (Gavrilović, Milanović-Pešić, Urošev 2012).

To validate the graphical interpretation, formal goodness-of-fit tests (K–S, CvM and χ^2) were conducted (Table 6).

At the Brus station, the K–S test indicates acceptable agreement at the 0.05 significance level for LN, GUM, PIII, and LPIII distributions, with LPIII providing the best fit (D_{max} = 0.063). At Bivolje station, all distributions showed acceptable agreement, with PIII providing the best fit (D_{max} = 0.100).

Furthermore, the CvM goodness-of-fit test confirm that the LPIII distribution provides the best overall fit to the data at the Brus station, followed by the PIII and LN distributions. The N distribution is rejected as inadequate, while the GUM distribution may be considered, though it is not optimal. At the Bivolje station, all tested distributions yielded *p*-values greater than 0.05, indicating that the null hypothesis cannot be rejected. Among these, the PIII distribution produced the lowest w^2 statistic and the highest *p*-value, suggesting it most closely aligns with the empirical data. LN, GUM and LPIII are also acceptable alternatives at this station.

The χ^2 test further supports these findings. At the Brus station, the LPIII distribution showed the highest agreement with the empirical data, while at the Bivolje station, the PIII distribution showed the best fit. According to the χ^2 statistics, both stations exhibit favorable correspondence with four tested theoretical distributions: LN, GUM, PIII, and LPIII.

A key objective of the FFA is to determine the quantile in the extreme upper tail of the best-fit distribution. Return level plots were generated using the PIII

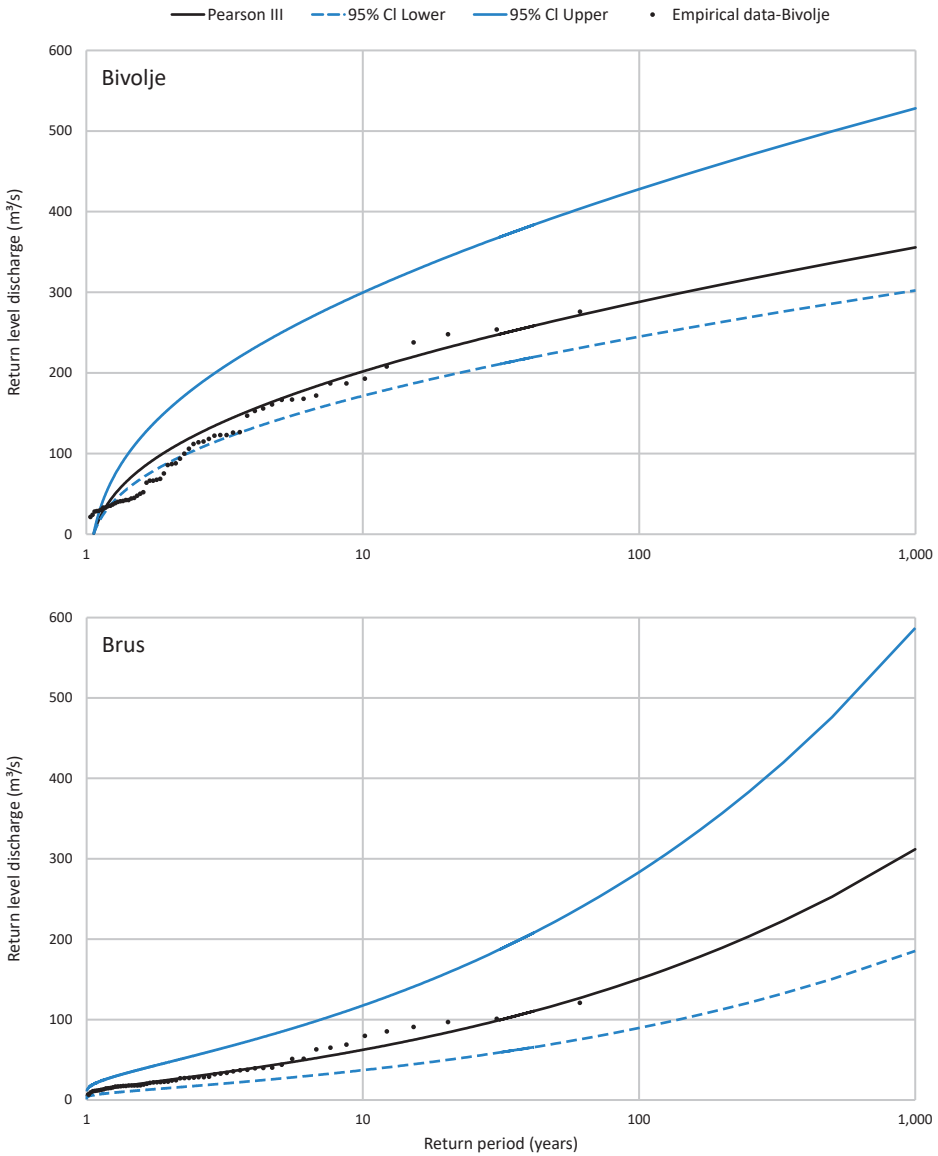

Fig. 5 – Estimated at-site return levels with 95% confidence bounds for the Brus (LPIII) and Bivolje (PIII) gauging stations in the Rasina River basin

distribution for the Bivolje station and the LPIII distribution for the Brus station, based on AMS. The empirical data closely follow the model lines of these distributions, indicating a good fit between the observed discharge data and the selected models. The LPIII distribution slightly better captures the higher

extremes due to the log-transformation, which is commonly applied in hydrological modeling. Using the quantile function and the parameter values specific to the best-fit distribution at each gauging station, we calculated the quantile estimates corresponding to return periods of 5, 10, 25, 50, 100, 200, 500, and 1,000 years, with 95% confidence intervals (Gnjato et al. 2025.). The 95% confidence intervals are relatively narrow for shorter return periods (up to approximately 100 years), reflecting greater certainty in these estimates. At Bivolje, empirical data show greater variability for longer return periods, indicating a less accurate fit of the PIII distribution. Wider confidence intervals than at Brus suggest increased uncertainty for rare extremes, likely due to local hydrology or limited data, warranting caution for long-term predictions (Fig. 5).

Based on the best-fitting theoretical distribution, the probability of exceedanceof maximum discharges (floods) in the Rasina River basin was calculated (Fig. 6). The maximum discharge of 121 m^3/s recorded at the Brus station corresponds to a probability of exceedanceof p = 2.38%, or a return period of approximately 42 years. At the Bivolje station, the maximum observed discharge corresponds to a probability of p = 2.35%, or a return period of 42.5 years. The annual maximum discharge with a 99.9% probability at Brus is approximately 4.3 m^3/s, while for a 90% probability it is around 11.6 m^3/s. At Bivolje, the corresponding discharges are 14.2 m^3/s (99.9%) and 31.3 m^3/s (90%), respectively.

The analysis demonstrates increasing discharge values across different return periods. These findings underscore the importance of accurate probability distributions in estimating extreme flood magnitudes, which are essential for effective risk management strategies in the Rasina River basin.

Conclusions

In this study, the FFA method based on L-moments was applied using various theoretical distributions fitted to AMS flow records from two hydrological stations in the Rasina River basin. The aim was to determine the most appropriate distribution type for different data sets. To calculate the regional frequency of AMS flows (i.e., flood risk parameters), flood quantiles and return levels were estimated with a 95% confidence interval. The results show that the *Z*-statistics for all considered distributions (N, LN, GUM, PIII, and LPIII) is in good agreement with the test requirement ($|Z| < 1.96$) at both stations. Since the absolute value of *Z* to the LPIII distribution is the lowest ($Z = 0.09$), this provides additional evidence that this distribution is suitable for the Rasina River basin as a whole.

Goodness-of-fit tests, including K–S, CvM and χ^2 identified the most suitable probability distributions for modeling river discharge maxima. At the Brus station, the LPIII distribution showed the highest agreement with empirical data, while

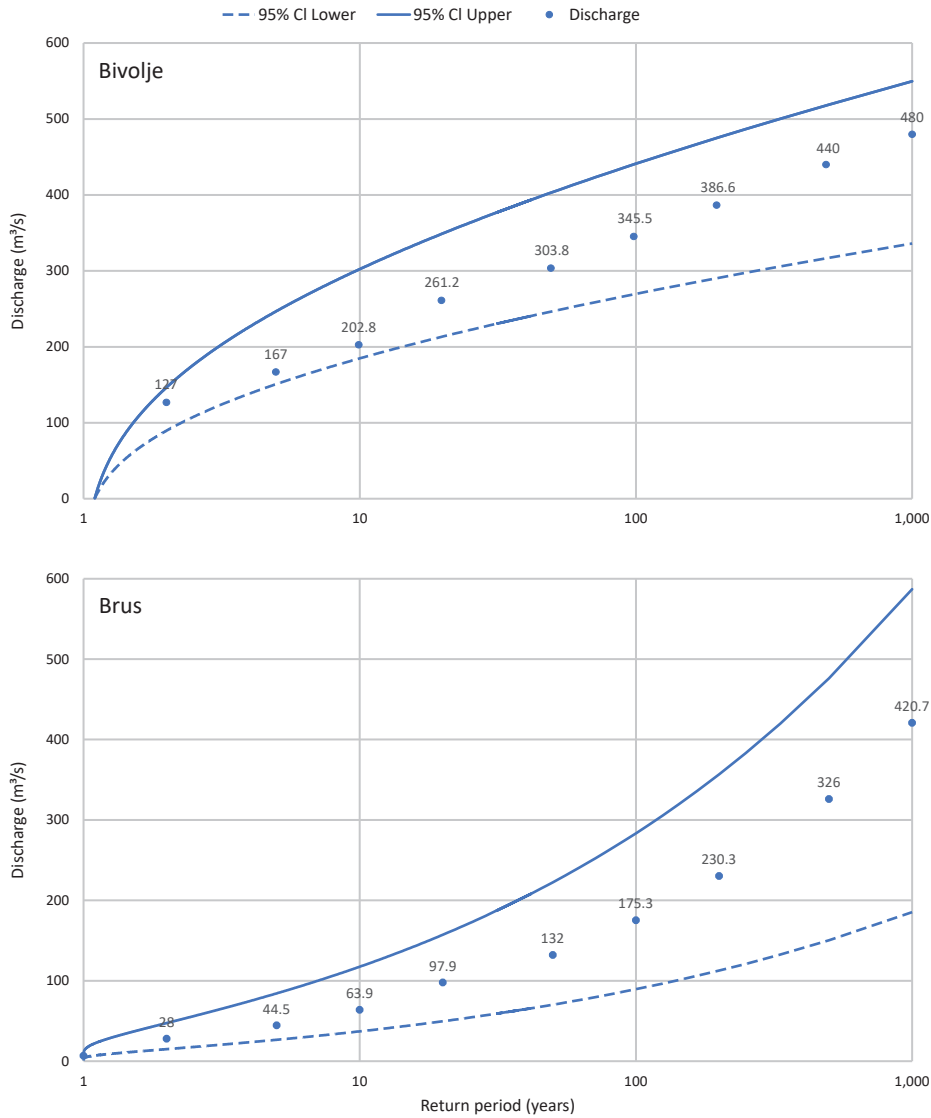

Fig. 6 – Estimated return discharge levels for different return periods for the Brus and Bivolje gauging stations in the Rasina River basin

at the Bivolje station, the PIII distribution provided the best fit. CDF diagrams visually confirmed these results, and the calculated return periods for extreme flood events offered valuable insights into potential runoff magnitudes for different return intervals. The evaluated time series (1961–2020) is sufficiently long and representative for the applied statistical indicators and for the analysis of

annual maximum discharges. The MK test indicated a decreasing trend in water discharge, with a statistically significant negative trend at Bivolje (Sen's slope –1.28 m^3/s/year).

Extreme flows at the upstream Brus station remained relatively stable throughout the observation period, reflecting near-natural flow conditions in the upper basin. Observed trends in extreme flows are generally consistent with long-term changes in mean and seasonal discharges reported in the literature for the Rasina River and comparable basins in Serbia and southeast Europe (Stričević, Martić-Bursać, Gocić 2024; Leščešen et al. 2022; Kovačević-Majkić, Urošev 2014). At the Bivolje station, decreasing extreme flows correspond with reported declines in average and seasonal discharges, whereas at the Brus station, minor fluctuations primarily reflect natural hydrological variability.

The differences between the two gauging stations reflect both natural variability and local catchment characteristics, including water regulation and abstraction in the upper and middle parts of the basin related to the Ćelije and Paljevštica water supply systems, as well as spatial variability in precipitation and runoff generation. Similar behavior has been documented in regional studies, which indicate that regulated river sections and smaller catchments often exhibit stronger negative trends and higher variability in extreme flows compared to less influenced or near-natural river reaches (Gnjato et al. 2025; Milanović-Pešić et al. 2025). This study provides detailed information on hydrological variable trends and flood estimation along the Rasina River basin over recent decades, which is useful for future regional and local planning and the integrated use of water resources. The results of this study offer valuable insights that enable more reliable estimation of design discharges for different return periods when designing hydraulic structures, potentially reducing the risk of failure and minimizing environmental damage and losses caused by future floods. An adequate combination of scientific analysis, hydro-construction works, and preventive measures is essential to ensure effective management and optimal protection of flood-affected areas in Serbia.

References

ACHARYA, B., JOSHI, B. (2020): Flood frequency analysis for an ungauged Himalayan river basin using different methods: a case study of Modi Khola, Parbat, Nepal. Meteorology Hydrology and Water Management, 8, 2, 46–51. https://doi.org/10.26491/mhwm/131092

AHMAD, I., FAWAD, M., AKBAR, M., ABBAS, A. (2016): Regional frequency analysis of annual peak flows in Pakistan using linear combination of order statistics. Polish Journal of Environmental Studies,, 25, 6, 1–10. https://doi.org/10.15244/pjoes/63782

ALFIERI, L., BISSELINK, B., DOTTORI, F., NAUMANN, G., ROO, A., SALAMON, P., WYSER, K., FEYEN, L. (2017): Global projections of river flood risk in a warmer world. Earth's Future, 5, 171–182. https://doi.org/10.1002/2016EF000485

ALFIERI, L., FEYEN, L., SALAMON, P., THIELEN, J., BIANCHI, A., DOTTORI, F., BUREK, P. (2016): Modelling the socio-economic impact of river floods in Europe, Natural Hazards and Earth System Sciences, 16, 1401–1411. https://doi.org/10.5194/nhess-16-1401-2016

AMIRATAEE, B., MONTASERI, M. (2013): Evaluation of L-moment and ppcc method to determine the best regional distribution of monthly rainfall data: case study northwest of Iran. Journal of Urban and Environmental Engineering, 7, 2, 247–252. https://doi.org/10.4090/juee.2013.v7n2.247-252

ANDERSON, S.T. (2019): Statistical L-moment and L-moment ratio estimation and their applicability in network analysis. PhD Dissertation, ir Force Institute of Technology, Wright-Patterson Air Force Base, Ohio, USA.

ANGHEL, C.G., ILINCA, C. (2023): Predicting flood frequency with the LH-moments method: a case study of Prigor River, Romania. Water, 15, 1–33. https://doi.org/10.3390/w15112077

ANWAT, K.V., HIRE, S.P., PAWAR, V.U., GUNJAL, P.R. (2021): Analysis of magnitude and frequency of floods in the Damanganga basin: western India. Hydrospatial Analysis, 5, 1, 1–11. https://doi.org/10.21523/gcj3.2021050101

ARNELL, W.N., GOSLING, N.S. (2014): The impacts of climate change on river flood risk at the global scale. Climatic Change, 1–16. https://doi.org/10.1007/s10584-014-1084-5

BAUER, K., SAGA Development Team (2020): System for Automated Geoscientific Analyses (SAGA) – GIS software, http://www.saga-gis.org (18. 1. 2026).

BERTOLA, M., VIGLIONE, A., LUN, D., HALL, J., BLOSCHL, G. (2020): Flood trends in Europe: are changes in small and big floods different? Hydrology and Earth System Sciences, 24, 1805–1822. https://doi.org/10.5194/hess-24-1805-2020

BEZAK, N., BRILLY, M., ŠRAJ, M. (2016): Flood frequency analyses, statistical trends and seasonality analyses of discharge data: a case study of the Litija station on the Sava River. Journal of Flood Risk Management, 9, 2, 154–168. https://doi.org/10.1111/jfr3.12118

BLOSCHL, G., HALL, J., VIGLIONE, A., PERDIGAO, R. A. P., PARAJKA, J., MERZ, B., LUN, D., ARHEIMER, B., ARONICA, G. T., BILIBASHI, A. (2019): Changing climate both increases and decreases European river floods. Nature, 573, 108–111. https://doi.org/10.1038/s41586-019-1495-6

CORINE Land Cover database (CLC2012), European Commission.

DERAMAN, W.H.A.W., ABD MUTALIB, N.J., MUKHTAR, Z.N. (2017): Determination of return period for flood frequency analysis using normal and related distributions. IOP Conf. Series: Journal of Physics: Conf. Series 890, 1, 1–11. https://doi.org/10.1088/1742-6596/890/1/012162

DIMITRIJEVIĆ, LJ. (2010): Hydro-geographical study of the Rasina River, Master thesis, Faculty of Geography, University of Belgrade.

DOMANSKI, P.D., JANKOWSKI, R., DZIUBA, K., GORA, R. (2023): Assessing control sustainability using L-moment ratio diagrams. Electronics, 12, 2377, 1–19. https://doi.org/10.3390/electronics12112377

DUBEY, A. (2014): Regional flood frequency analysis utilizing L-moments: a case study of Narmada basin. International Journal of Engineering Research and Applications, 155–161.

ENGELAND, K., WILSON, D., BORSANYI, P., ROALD, L., HOLMQVIST, E. (2018): Use of historical data in flood frequency analysis: a case study for four catchments in Norway. Hydrology Research, 49, 2, 466–486. https://doi.org/10.2166/nh.2017.069

ENGLAND, F.J., COHN, A.T., FABER, A.B., STEDINGER, R.J., THOMAS, O.W., BAKER, M., VEILLEUX, G.A., KIANG, E.J., MASON, R.R. (2019): Guidelines for determining flood flow frequency–Bulletin 17C. U.S. Geological Survey Techniques and Methods, book 4, U. S. Geological Survey, Reston, Virginia. https://doi.org/10.3133/tm4B5

FISCHER, S., SCHUMANN, A.H. (2021): Multivariate flood frequency analysis in large river basins considering tributary impacts and flood types. Water Resources Research, 57, 1–25. https://doi.org/10.1029/2020WR029029

GAVRILOVIĆ, LJ. (1981): Floods in Serbia in the 20th century: causes and consequences. Special issues, 52. Serbian Geographical Society, Belgrade.

GAVRILOVIĆ, LJ., DUKIĆ, D. (2002): Rivers of Serbia. Serbian State of Textbooks, Belgrade.

GAVRILOVIĆ, LJ., MILANOVIĆ-PEŠIĆ, A., UROŠEV, M. (2012): A hydrological analysis of the greatest floods in Serbia in the 1960–2010 period. Carpathian Journal of Earth and Environmental Sciences, 7, 4, 107–116.

GIELCZEWSKI, M., PINIEWSKI, M., DOMANSKI, P. (2022): Mixed statistical and data mining analysis of river flow and catchment properties at regional scale. Stochastic Environmental Research and Risk Assessment, 36, 2861–2882. https://doi.org/10.1007/s00477-022-02169-3

GNJATO, S., LEŠČEŠEN, I., POPOV, T., TRBIĆ, G. (2025): Comprehensive flood frequency analysis of major Sava River affluents in Bosnia and Herzegovina: risks, and implications for water resources management. IDŐJÁRÁS, 129, 2, 161–175. https://doi.org/10.28974/idojaras.2025.2.3

GREENWOOD, J.A., LANDWEHR, J.M., MATALAS, N.C., WALLIS, J.R. (1979): Probability weighted moments: definition and relation to parameters of several distributions expressable in inverse form. Water Resources Research, 15, 5, 1049–1054. https://doi.org/10.1029/WR015i005p01049

HALL, J., BLOSCHL, G. (2018): Spatial patterns and characteristics of flood seasonality in Europe. Hydrology and Earth System Sciences, 22, 3883–3901. https://doi.org/10.5194/hess-22-3883-2018

HIGASHINO, M., STEFAN, G.H. (2019): Variability and change of precipitation and flood discharge in a Japanese river basin. Journal of Hydrology: Regional Studies, 21, 68–79. https://doi.org/10.1016/j.ejrh.2018.12.003

HOSKING, J.R.M. (1990): L-moments: Analysis and Estimation of Distributions using Linear Combinations of Order Statistics. Journal of the Royal Statistical Society: Series B, 52, 1, 105–124. https://doi.org/10.1111/j.2517-6161.1990.tb01775.x

HOSKING, J.R.M., WALLIS, J.R. (1993): Some statistics useful in regional frequency analysis. Water Resources Research, 29, 2, 271–281. https://doi.org/10.1029/92WR01980

HOSKING, J.R.M., WALLIS, J.R. (1997): Regional frequency analysis: an approach based on L-moments. Cambridge University Press, UK. https://doi.org/10.1017/CBO9780511529443

HU, L., NIKOLOPOULOS, E.I., MARRA, F., ANAGNOSTOU, E.N. (2023): Toward an improved estimation of flood frequency statistics from simulated flows. Journal of Flood Risk Management, 16, 2, 1–13. https://doi.org/10.1111/jfr3.12891

ILINCA, C., ANGHEL, C.G. (2022): Flood-frequency analysis for dams in Romania. *Water*, 14, 18, 1–23. https://doi.org/10.3390/w14182884

IONITA, M., NAGAVCIUC, V. (2021): Extreme floods in the eastern part of Europe: large-scale drivers and associated impacts. Water, 1122, 1–26. https://doi.org/10.3390/w13081122

JONKMAN, S.N., CURRAN, A., BOUWER L.M. (2024): Floods have become less deadly: an analysis of global flood fatalities 1975–2022. Natural Hazards, 120, 6327–6342. https://doi.org/10.1007/s11069-024-06444-0

KENDALL, M.G. (1975): Rank correlation methods, 4th ed. Charles Griffin, London.

KHAN, Z., RAHMAN, A., KARIM, F. (2023): An assessment of uncertainties in flood frequency estimation using bootstrapping and Monte Carlo simulation. Hydrology, 10, 1–16. https://doi.org/10.3390/hydrology10010018

KOUSAR, S., KHAN, R.A., HASSAN, U.M., NOREEN, Z., BHATTI, H.S. (2020): Some best-fit probability distributions for at-site flood frequency analysis of the Ume River. Journal of FloodRisk Management, 13, 1–11. https://doi.org/10.1111/jfr3.12640

KOVAČEVIĆ, M., MARKOVIĆ, LJ., BABIĆ, L. (2014): Statistical modeling of extreme values: application to calculate extreme flow at River Rasina. Construction Materials and Structures, 57, 4, 21–29. https://doi.org/10.5937/grmk1404021K

KOVAČEVIĆ-MAJKIĆ, J., UROŠEV, M. (2014): Trends of mean annual and seasonal discharges of rivers in Serbia. Journal of the Geographical Institute "Jovan Cvijić" SASA, 64, 2, 143–160. https://doi.org/10.2298/IJGI1402143K

LEHMKUHL, F., SCHUTTRUMPF, H., SCHWARZBAUER, J., BRULL, C., DIETZE, M., LETMATHE, P., VOLKER, C., HOLLERT, H. (2022): Assessment of the 2021 summer flood in central Europe. Environmental Sciences Europe, 34, 1, 1–6. https://doi.org/10.1186/s12302-022-00685-1

LEŠČEŠEN, I., DOLINAJ, D. (2019): Regional flood frequency analysis of the Pannonian Basin. Water, 11, 1–15. https://doi.org/10.3390/w11020193

LEŠČEŠEN, I., ŠRAJ, M., BASARIN, B., PAVIĆ, D., MESAROŠ, M., MUDELSEE, M. (2022): Regional flood frequency analysis of the Sava River in south-eastern Europe. Sustainability, 14, 9282, 1–19. https://doi.org/10.3390/su14159282

MANN, H.B. (1945): Non-parametric tests against trend. Econometrica, 13, 245–259. https://doi.org/10.2307/1907187

MARTIĆ-BURSAĆ, N., STRIČEVIĆ, LJ., NIKOLIĆ, M., IVANOVIĆ, R. (2016): Statistical analysis of average, high and low waters of the Toplica River. Bulletin of the Serbian Geographical Society, 96, 1, 26–45. https://doi.org/10.2298/GSGD1601026M

MARTINENKO, A., JEVREMOVIĆ, V., VRANIĆ, P., POPOVIĆ, J., PEJIĆ, M. (2021): Statistical tests and their application in geodesy. Technology, Our Civil Engineering, 75, 147–154. https://doi.org/10.5937/tehnika2102147M

MASSERONI, D., CAMICI, S., CISLAGHI, A., VACCHIANO, G., MASSARI, C., BROCCA, L. (2021): The 63-year changes in annual streamflow volumes across Europe with a focus on the Mediterranean basin. Hydrology and Earth System Sciences, 25, 5589–5601. https://doi.org/10.5194/hess-25-5589-2021

MILANOVIĆ-PEŠIĆ, A. (2020). Hydrological aspects of the floods in the Kolubara River basin (Serbia) – analyses and flood mitigation measures. In: Nedkov, S. et al. (eds.): Smart Geography. Springer, Cham, 117–127. https://doi.org/10.1007/978-3-030-28191-5_10

MILANOVIĆ-PEŠIĆ, A., JAKOVLJEVIĆ, D., RAJČEVIĆ, V., GNJATO, S. (2025): Assessment of hydroclimatic trends in southeast Europe – examples from two adjacent countries (Bosnia & Herzegovina and Serbia). Időjárás, 129, 1, 69–87. https://doi.org/10.28974/idojaras.2025.1.5

MORLOT, M., BRILLY, M., ŠRAJ, M. (2019): Characterisation of the floods in the Danube River basin through flood frequency and seasonality analysis. Acta Hydrotechnica, 32, 57, 73–89. https://doi.org/10.15292/acta.hydro.2019.06

NOTO, L., LA LOGGIA, G. (2009): Use of L-moments approach for regional flood frequency analysis in Sicily, Italy. Water Resources Management, 23, 2207–2229. https://doi.org/10.1007/s11269-008-9378-x

PARAJKA, J., KOHNOVAB, S., BALINTH, G., BARBUCF, M., BORGAE, M., CLAPSI, P., CHEVALD, S., DUMITRESCUD, A., GAUMEC, E., HLAVCOVAB, K., MERZA, R., PFAUNDLERG, M., STANCALIED, G., SZOLGAYB, J., BLOSCHLA, G. (2010): Seasonal characteristics of flood regimes across the Alpine–Carpathian range. Journal of Hydrology, 394, 1–2, 1–13. https://doi.org/10.1016/j.jhydrol.2010.05.015

PETROVIĆ, A.M., LEŠČEŠEN, I., RADEVSKI, I. (2024): Unveiling torrential flood dynamics: a comprehensive study of spatio-temporal patterns in the Šumadija Region, Serbia. Water, 16, 7, 991, 1–19. https://doi.org/10.3390/w16070991

QGIS Development Team (2023): Quantum GIS (QGIS) 3.40. Open-source GIS software for spatial data entry, analysis and visualization. https://qgis.org (18. 1. 2026).

RADEVSKI, I., GORIN, S. (2017): Floodplain analysis for different return periods of river Vardar in Tikvesh valley (Republic of Macedonia). Carpathian Journal of Earth and Environmental Sciences, 12, 1, 179–187.

RADEVSKI, I., GORIN, S., TALESKA, M., DMITROVSKA, O. (2018): Natural regime of streamflow trends in Macedonia. Geografie, 123, 1–20. https://doi.org/10.37040/geografie2018123010001

RAHMAN, A.S., RAHMAN, A., ZAMAN, M.A., HADDAD, K., AHSAN, A., IMTEAZ, M. (2013): A study on selection of probability distributions for at-site flood frequency analysis in Australia. Natural Hazards, 69, 3, 1803–1813. https://doi.org/10.1007/s11069-013-0775-y

RHMSS (2023): Republic Hydrometeorological Service of Serbia, https://www.hidmet.gov.rs/ (10. 12. 2024).

SAHU, R., KANT VERMA, M., AHMAD, I. (2022): Regional frequency analysis using L-moment methodology – a eview, In: Pathak, K.K. et al. (eds.): Recent trends in civil engineering. Springer Nature Singapore Pte Ltd., Singapore, 811–832. https://doi.org/10.1007/978-981-15-5195-6_60

SAMANTARAY, S., SAHOO, A. (2020): Estimation of flood frequency using statistical method: Mahanadi River basin, India. H2Open Journal, 3, 1, 189–207. https://doi.org/10.2166/h2oj.2020.004

SEN, P.K. (1968): Estimates of the regression coefficient based on Kendall's tau. Journal of the American Statistical Association, 63, 324, 1379–1389. https://doi.org/10.1080/01621459.1968.10480934

SHAH, I.A., PAN DAS, N. (2024): Evaluation of probability distribution methods for flood frequency analysis in the Jhelum basin of north-western Himalayas, India. Cleaner Water, 2, 1–14. https://doi.org/10.1016/j.clwat.2024.100044

SMITH, A., SAMPSON, C., BATES, P. (2015): Regional flood frequency analysis at the global scale. WaterResources Researsh, 51, 539–553. https://doi.org/10.1002/2014WR015814

SNIZHKO, S., BERTOLA, M., OVCHARUK, V., SHEVCHENKO, O., DIDOVETS, I., BLOSCHL, G. (2023): Climate impact on flood changes – an Austrian-Ukrainian comparison. Journal of Hydrology and Hydromechanics, 71, 3, 271–282. https://doi.org/10.2478/johh-2023-0017

SORS (2021): Statistical Office of the Republic of Serbia. http://www.stat.gov.rs (5. 7. 2025).

STAGL, J., HATTERMANN, F. (2015): Impacts of climate change on the hydrological regime of the Danube River and Its tributaries using an ensemble of climate scenarios. Water, 7, 6139–6172. https://doi.org/10.3390/w7116139

STOJKOVIĆ, M., KOSTIĆ, S., PROHASKA, S., PLAVŠIĆ, J., TRIPKOVIĆ, V. (2017): A new approach for trend assessment of annual streamflows: a case study of hydropower plants in Serbia. Water Resources Management, 31, 4, 1089–1103. https://doi.org/10.1007/s11269-017-1583-z

STRIČEVIĆ, LJ. (2015): Water resources of Rasina county and their impact on regional development. PhD thesis, Faculty of Sciences and Mathematics, University of Niš.

STRIČEVIĆ, LJ., MARTIĆ-BURSAĆ, N., GOCIĆ, M. (2024): Trend analysis of temperature, precipitation and river discharge in the Rasina river basin, Serbia. VI Congress of Macedonian Geographers with International Participation, Macedonian Geographical Society, 29.–30. 5. 2024. https://doi.org/10.37658/MGD24021s

TRAMBLAY, Y., MIMEAU, L., NEPPEL, L., VINET, F., SAUQUET, E. (2019): Detection and attribution of flood trends in Mediterranean basins. Hydrology and Earth System Sciences, 23, 4419–4431. https://doi.org/10.5194/hess-23-4419-2019

UNDRR (2025): Floods. In: Global Assessment Report 2025. United Nations Office for Disaster Risk Reduction, https://www.undrr.org/gar/gar2025/hazard-exploration/floods (10. 5. 2024).

UROŠEV, M., LEŠČEŠEN, I., ŠTRBAC, D., DOLINAJ, D. (2016): Extreme hydrological situations on Danube River: Case study Bezdan Hydrological Station (Serbia). In Proceedings of the 4th IAHR European Congress, Liège, Belgium. International Association for Hydro-Environment Engineering and Research.

USGS (n.d.): SRTM Digital Elevation Data, https://www.earthexplorer.usgs.gov (18. 1. 2026).

VARLAS, G., PAPADAKI, C., STEFANIDIS, K., MENTZAFOU, A., PECHLIVANIDIS, I., PAPADOPOULOS, A., DIMITRIOU, E. (2023): Increasing trends in discharge maxima of a Mediterranean River during early autumn. Water, 15, 1022. https://doi.org/10.3390/w15061022

VASILEVSKI, D., RADEVSKI, I. (2014): Analysis of high waters on the Kriva Reka River, Macedonia, Acta Geographica Slovenica, 54, 2, 363–377. https://doi.org/10.3986/AGS54209

VUJOVIĆ, R. (1995): Waters of Serbia – development plans and several realizations in water management. IRO Building Book, Belgrade.

ZAKARIA, Z.A., SHABRI, A. (2013): Regional frequency analysis of extreme rainfalls using partial L-moments method. Theoretical and Applied Climatology, 113, 1–2, 83–94. https://doi.org/10.1007/s00704-012-0763-2

ACKNOWLEDGEMENTS

This work was supported by the Ministry of Education, Science and Technological Development of the Republic of Serbia (Agreement No 451–03-137/2025–03/ 200124), Faculty of Sciences and Mathematics, University of Niš.

ORCID

LJILJANA STRIČEVIĆ
https://orcid.org/0000-0002-0574-2009

NATAŠA MARTIĆ-BURSAĆ
https://orcid.org/0000-0002-9142-8509

MILENA GOCIĆ
https://orcid.org/0000-0003-1490-0838

NIKOLA MILENTIJEVIĆ
https://orcid.org/0000-0003-4450-844X

MARKO IVANOVIĆ
https://orcid.org/0000-0001-5281-4776